energies

MDPI

Article

Crushing of Single-Walled Corrugated Board during Converting: Experimental and Numerical Study

Tomasz Garbowski [1], Tomasz Gajewski [2,*], Damian Mrówczyński [3] and Radosław Jędrzejczak [4]

[1] Department of Biosystems Engineering, Poznan University of Life Sciences, Wojska Polskiego 50, 60-627 Poznań, Poland; tomasz.garbowski@up.poznan.pl
[2] Institute of Structural Analysis, Poznan University of Technology, Piotrowo 5, 60-965 Poznań, Poland
[3] R&D Department, FEMat Sp. z o.o., Romana Maya 1, 61-371 Poznań, Poland; damian.mrowczynski@fematproject.pl
[4] Werner Kenkel Sp. z o.o., Mórkowska 3, 64-117 Krzycko Wielkie, Poland; radoslaw.jedrzejczak@wernerkenkel.com.pl
* Correspondence: tomasz.gajewski@put.poznan.pl

Abstract: Corrugated cardboard is an ecological material, mainly because, in addition to virgin cellulose fibers also the fibers recovered during recycling process are used in its production. However, the use of recycled fibers causes slight deterioration of the mechanical properties of the corrugated board. In addition, converting processes such as printing, die-cutting, lamination, etc. cause micro-damage in the corrugated cardboard layers. In this work, the focus is precisely on the crushing of corrugated cardboard. A series of laboratory experiments were conducted, in which the different types of single-walled corrugated cardboards were pressed in a fully controlled manner to check the impact of the crush on the basic material parameters. The amount of crushing (with a precision of 10 micrometers) was controlled by a precise FEMat device, for crushing the corrugated board in the range from 10 to 70% of its original thickness. In this study, the influence of crushing on bending, twisting and shear stiffness as well as a residual thickness and edge crush resistance of corrugated board was investigated. Then, a procedure based on a numerical homogenization, taking into account a partial delamination in the corrugated layers to determine the degraded material stiffness was proposed. Finally, using the empirical-numerical method, a simplified calculation model of corrugated cardboard was derived, which satisfactorily reflects the experimental results.

Keywords: corrugated cardboard; converting; numerical homogenization; strain energy equivalence; finite element method; shell structures; transverse shear

Citation: Garbowski, T.; Gajewski, T.; Mrówczyński, D.; Jędrzejczak, R. Crushing of Single-Walled Corrugated Board during Converting: Experimental and Numerical Study. *Energies* **2021**, *14*, 3203. https://doi.org/10.3390/en14113203

Academic Editor: Peter Foot

Received: 6 May 2021
Accepted: 27 May 2021
Published: 30 May 2021

1. Introduction

Paper and cardboard are made of cellulose fibers that mainly come from trees. Some of the fibers circulate repeatedly in the production-recycling loop. The material is, therefore, environmentally friendly, but the quality of the produced material from recycled fibers iteratively declines. This requires a deeper understanding if one wants to optimize the product and at the same time keep the material eco-friendly. It becomes even more important if the final product is a corrugated cardboard, which consists of two to seven alternating flat (liners) and corrugated (fluting) layers of paperboard.

The particular orientation of the fibers resulting from the cardboard production process causes the material to have different mechanical properties along the mutually perpendicular directions. Such materials are called orthotropic materials, as opposed to isotropic ones, which exhibit the same physical properties independent of the direction. The material orientation along the fibers that follow the direction of the web during production is called the machine direction (MD), the direction perpendicular to it is called the cross direction (CD). As the material is much stiffer and stronger in MD (along fibers), the corrugated board production method compensates for its poorer behavior in CD by using the corrugated

layers. The main task of which is to increase the load capacity and stiffness in the CD, but most importantly, to keep the flat layers at an appropriate distance from each other, which allows obtaining significantly increased bending stiffness in both directions.

The optimal corrugated board should be characterized by maximum strength and stiffness, and at the same time be light and cheap to produce. In assessing the quality of corrugated board, the compressive or tensile and flexural or torsional stiffnesses/strengths are important; the former due to the load-bearing capacity, while the latter due to the resistance to loss of stability. The maximum stiffness or strength can be obtained by selecting the appropriate materials for the individual layers and/or by selecting the appropriate geometry (wave height and period) for the corrugated layers. There are hundreds of papers on the market with different grammages and mechanical properties, produced in a different proportion of virgin to recycled fibers. This gives an enormous number of combinations of possible layer arrangements and layer geometry of the corrugated cardboard, which does not stop producers from constantly trying to find the best solution. Unfortunately, their efforts may be wasted if the carefully designed quality of the corrugated cardboard does not achieve the assumed strength parameters after production, i.e., converting processes.

Before corrugated board becomes a typical transportation box, or a color, branded shelf-ready box (SRP) or a display-ready box it goes through a number of converting processes, e.g., printing, lamination, die-cutting, etc. All these processes cause crushing of the corrugated layers, which in turn leads to a reduction of strength and stiffness of the material and therefore affects the performance of structures made of corrugated boards. The deterioration of the mechanical properties can be observed in all crucial laboratory test results, e.g., four-point bending test, torsional test, shear test, edge crush test, etc. Even though, the degraded stiffnesses and strengths could easily be measured by cutting specimens from the converted cardboard, this is rarely done in practice. Typically, this effect is accounted for by adding safety factors to the equations that estimate the load capacity of the package.

Since the middle of the last century, scientists and engineers have tried to find robust and simple tools for estimating the strength of corrugated board boxes. Among them the analytical tools [1–10] are the simplest, but unfortunately less precise and limited only to the typical box structures. Numerical models of corrugated board packaging [11–16], although much more precise, require specific knowledge and a full set of material parameters to correctly simulate the behavior of the box.

In the finite element-based tools, a procedure called homogenization [17–25] is very often used, which allows for significant time savings in the analysis and at the same time guarantees the correct behavior of simplified models. This is especially important when the computational models are complex (they consist of many layers of cardboard) or the analysis concerns geometries with complex shapes, such as cardboard furniture [26].

In our previous works, we presented analytical-numerical methods [27–29] for assessing the strength of corrugated board boxes, which allow to obtain quick and accurate results for the packaging with different geometries (ventilation/hand holes [28] and perforations [29]). In order to properly estimate the strength of a corrugated box, special attention should be paid to transverse shear properties [30–32]. This is because the decrease in this material parameter significantly affects the load-bearing capacity of the package. In general, any deteriorated stiffness (i.e., flexural, torsional or transversal) and the strength of the corrugated board can be readily implemented in any estimation method. The only requirement is to determine the relationship between the amount of damage (stiffness and strength degradation) and the amount of physical crushing of the cardboard.

The article presents the results of the research on the crushing of various single-walled corrugated boards. In the first step, the relationship between intentionally induced crushing with very high accuracy to different types of corrugated boards and the measured loss of stiffness in various laboratory tests was checked. Since the crushing of the sample takes place in the thickness direction, the greatest decrease in bending and twisting stiffness (due to the reduction of the corrugated board thickness and, therefore, a significant reduction of

the section moment of inertia) was expected. Less load capacity reduction was expected in the edge crush test. However, due to the high resilience of the corrugated board, in some cases, especially for a small amount of crushing, the sample recovers its original thickness (because of the relaxation), which allow the observation of interesting findings. All issues will be discussed in the Results section.

In the second step, a numerical model based on the homogenization that can easily be used to predict all the stiffness parameters of the corrugated board with different degrees of crushing was proposed. The numerical model, based on the finite element method (FEM), was used to build a global stiffness matrix of the full detailed 3D finite element (FE) model of the corrugated board. The model (based on the numerical homogenization procedure presented in [25]) takes into account the crushing of the corrugated board. This extension of the homogenization procedure allows to determine the degraded corrugated board stiffness matrix, which ultimately enables a robust simulation of the real laboratory tests using the simplified analytical formulas. The results obtained from the simulation of four-point bending and torsion (twist) tests [31,32] are in good agreement with the results obtained from the laboratory tests.

2. Materials and Methods

2.1. Mechanical Tests of Corrugated Cardboard

The strength and stiffness of a corrugated board can be determined by performing various types of tests. The most commonly used include: (a) BNT—stiffness in the four-point bending test; (b) ECT—edge crush test, (c) SST—shear stiffness testing and (d) TST—torsional stiffness test.

The measurement of the bending stiffness is a laboratory test which is based on the four-point bending method (BNT), see Figure 1. This test is usually carried out on a sample with a dimension of 50 × 250 mm. It is important that in this test there is a constant moment and zero shear force in the sample between the internal supports. However, there is still a shear force between the outer and inner supports—this allows to take into consideration the shear stiffness aspect. It is worth noting that a bending stiffness measurement is very sensitive to sample damage (crushing or creasing), so the results for samples crushed by more than 50% are usually unreliable.

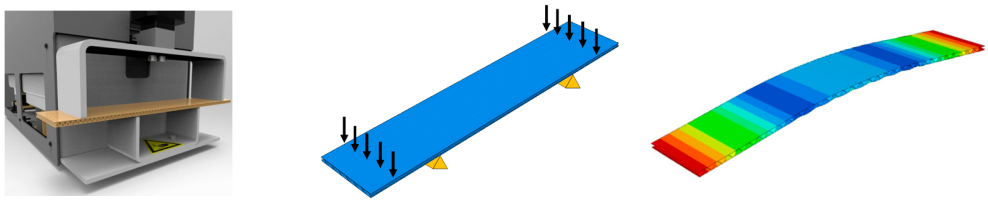

(**a**) (**b**) (**c**)

Figure 1. The four-point bending test: (**a**) cardboard testing device; (**b**) loaded sample; (**c**) deformed sample.

The sample compressive strength in the Edge Crush Test (ECT) is obtained for relatively stocky samples (conventionally thicker than 1 mm) with dimensions of 25 × 100 mm, see Figure 2. In the case of slender specimens, the main failure mechanism is the loss of stability, and not the crushing of a sample. The ECT of the corrugated cardboard is one of the most known and important (from the practical point of view) parameter, often used in an analytical [1,10] or an analytical-numerical [27–29] determination of the load capacity of a corrugated board packaging.

The shear stiffness (SST) of a corrugated board is measured on a sample 80 × 80 mm loaded with a pair of forces at opposite corners, see Figure 3. Measuring the displacements and reaction forces at the other two corners allows to determine the cardboard shear stiffness. Only the linear part of the load-displacement curve is used in an identification of the sample shear stiffness. The SST parameter is very sensitive to a sample

crushing. The results obtained in the SST laboratory tests are valid also for highly crushed or broken samples.

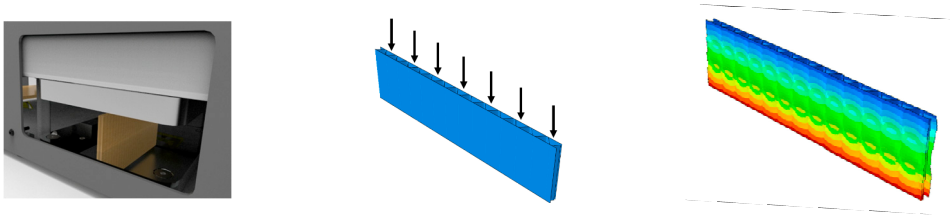

(**a**) (**b**) (**c**)

Figure 2. The edge crush test: (**a**) corrugated board testing device; (**b**) loaded sample; (**c**) deformed sample.

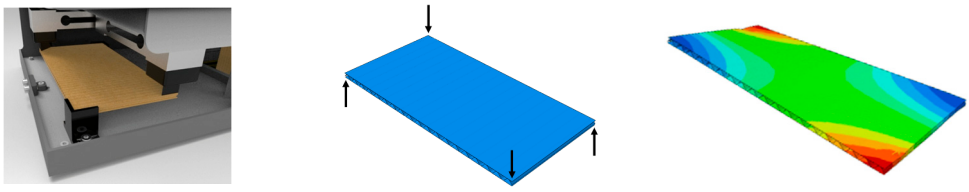

(**a**) (**b**) (**c**)

Figure 3. The shear stiffness testing: (**a**) cardboard testing device; (**b**) loaded sample; (**c**) deformed sample.

In the torsional stiffness (TST) measurement, a twisting of a 25 × 150 mm sample by a few degrees in both directions is conducted, see Figure 4. The results obtained are valid even for highly crushed or broken samples. Therefore, the TST parameter has a high sensitivity to crushing of the corrugated board sample. Only the linear part of a diagram (i.e., the angle of rotation vs bending moment) is used to determine the sample torsional stiffness. The reliable measurements are assured by: (1) a stable method of holding the sample, (2) a static method of measuring the angle of rotation and torque and (3) a relatively large width of the sample, thanks to which the sample behaves as a homogenized material.

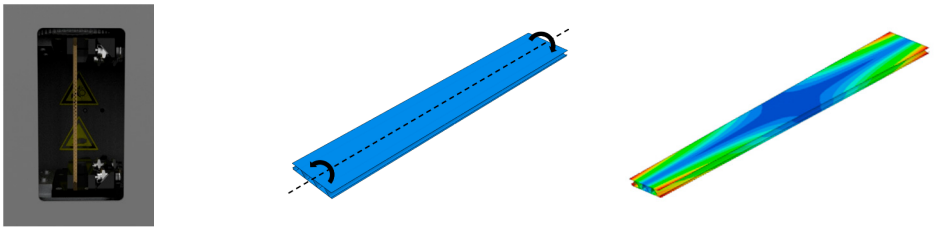

(**a**) (**b**) (**c**)

Figure 4. The torsional stiffness test: (**a**) cardboard testing device; (**b**) loaded sample; (**c**) deformed sample.

The crushing device (CRS) is used to assess the impact of converting processes such as laminating, stamping, creasing or printing on the quality and load-bearing capacity of the corrugated board, see Figure 5. In this research, a fully controlled manner of crushing cardboard in the range from 10% to 70% was precisely obtained by using the CRS laboratory device (fematsystems.pl/services/crs [33]), which assured the crushing accuracy of ±10 µm.

In Figures 1–5, the devices for different testing methods of corrugated cardboards are presented. Furthermore, the loading scheme of the sample (Figure 5b), as well as the

deformed shape of the sample (Figure 5c) with exemplary displacement fields (obtained via finite element method modelling and analytical approximation) are illustrated.

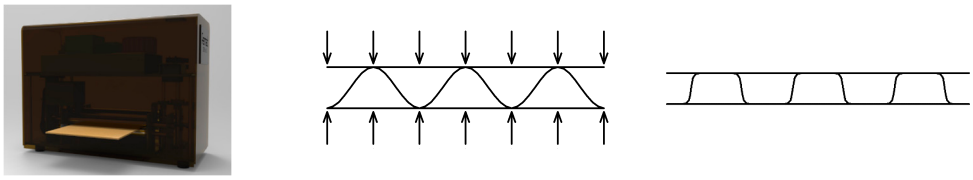

(**a**) (**b**) (**c**)

Figure 5. The cardboard crushing: (**a**) cardboard testing device; (**b**) loaded sample scheme; (**c**) deformed sample scheme.

2.2. Estimation Error by Coefficient of Determination

To explore the relationship between a crushing and a decrease of the corrugated board stiffness values, the coefficient of determination was computed for each board quality, defined by the formula:

$$R^2 = 1 - \frac{\sum_{i=1}^{n}(x_i - \hat{y}_i)^2}{(n-1)\cdot \mathrm{var}(x)}, \tag{1}$$

where: x_i—the expected ratio of the measured value of the crushed sample to the initial value ($\mathrm{CRS} = 0\% \rightarrow x_i = 1.0,\ \mathrm{CRS} = 10\% \rightarrow x_i = 0.9,$ etc.), $\hat{y}_i$—the values computed on the basis of the formula (2) describing the linear regression, $\mathrm{var}(x)$ — the variance of the expected ratio of the measured value of the crushed sample to the initial value:

$$\hat{y}_i = a(x_i - \overline{x}) + \overline{y}, \tag{2}$$

where: $\overline{x}$—the mean value of the expected ratio of the measured value of the crushed sample to the initial value, $\overline{y}$—the mean value of the measured quantities (SST-MD, TST-CD etc.), a—the slope of the linear regression:

$$a = \frac{\sum_{i=1}^{n}(x_i - \overline{x})(y_i - \overline{y})}{\sum_{i=1}^{n}(x_i - \overline{x})^2}. \tag{3}$$

The higher the value of the coefficient of determination, R^2, the better the fit of the regression line and the estimation error is considered to be smaller.

2.3. Numerical Approach for Modelling Crushing

In this paper, apart from laboratory tests on crushed corrugated cardboards, also a simple numerical approach to consider the crushed properties of the corrugated board is proposed. The derived method does not require the modelling of the plasticization of the fluting, because its analytical equivalent (presented later) in FE model can be used. The aim of this part of the study is to validate the approach by using torsion test modelling [31,32]. The numerical study consists of several steps, illustrated by scheme in Figure 6:

- Building initial geometry of the intact corrugated cardboard (stage a).
- Performing FE analysis of corrugated cardboard crushing with plasticity included (stage b)—substituted with an analytical, simplified crushed flute shape approximation.
- Using the crushed geometry to build the classical material stiffness matrix of corrugated cardboard (stage c,d).
- Homogenizing the crushed corrugated cardboard by composite properties, based on Garbowski and Gajewski method [25] (stage d,e).
- Computing torsion/bending response of crushed corrugated cardboard sample using composite properties (stage f).

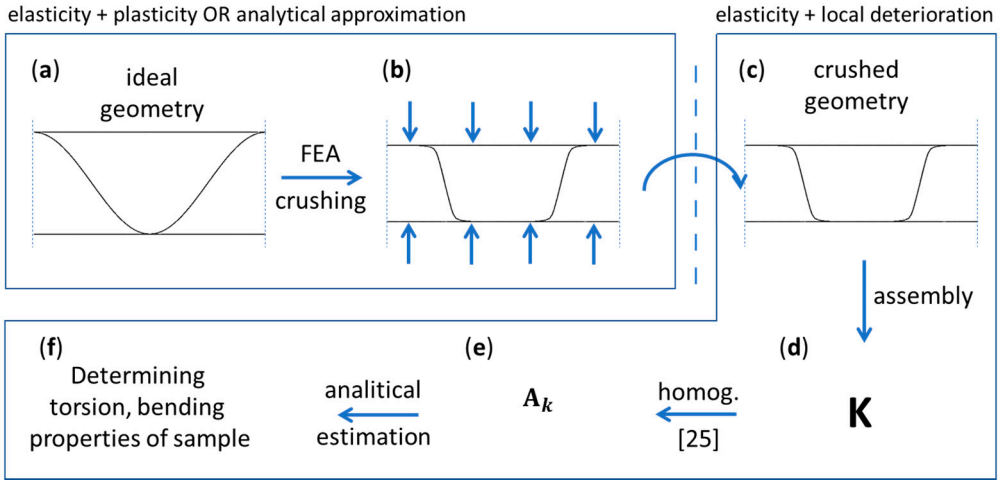

Figure 6. The scheme representing the steps of numerical study conducted in this study: (**a**) undeformed RVE, (**b**) loaded and deformed RVE, (**c**) crushed geometry extracted, (**d**) material stiffness matrix of RVE, (**e**) the representative shell stiffness matrix and (**f**) tests outcomes from analytical estimation.

Initial geometry of the corrugated cardboard used in the numerical study represents an intact (i.e., unconverted or uncrushed) geometry of the cardboard and it was assumed from the literature [19,25]. The fraction of a single wall corrugated cardboard was simulated, namely, the in-plane section of 8 × 8 mm. The fluting period was also 8 mm; the fluting wave "starts" from the liner. The thickness of the liners and fluting are 0.29 mm and 0.30 mm, respectively. The axial spacing between the liners is 3.51 mm.

The material parameters of intact corrugated cardboard were also taken from the literature [19,25]. The classical orthotropic constitutive law was assumed for each layer with a perfect plasticity (no hardening). The orthotropic material data (E_1, E_2, ν_{12}, G_{12}, G_{13} and G_{23}, i.e., Young moduli in both directions, Poisson's ratio and 3 shear moduli, respectively) and yield stress, σ_0, for liners and fluting are presented in Table 1.

Table 1. Material properties of liners and fluting of intact corrugated cardboard.

Layers	E_1	E_2	ν_{12}	G_{12}	G_{13}	G_{23}	σ_0
	(MPa)	(MPa)	(-)	(MPa)	(MPa)	(MPa)	(MPa)
liners	3326	1694	0.34	859	429.5	429.5	2.5
fluting	2614	1532	0.32	724	362	362	2.5

To acquire the crushed geometry of the corrugated cardboard the static FE analysis was performed. In the numerical study, five cases were considered, see Figure 7, in which the induced crushing of the cardboard were 10%, 20%, 30%, 40% and 50%. For instance, 10% of crushing means here that the corrugated cardboard was enforced by kinematic constraint to decrease its thickness to be 90% of the intact geometry (see Figure 6a,b). In the numerical model (to the upper and lower liner surfaces) the kinematic constraints were applied assuming that 50% of the crushed deformation is elastic and the other 50% comes from the plastic and/or damage deformations. Therefore, in the numerical analysis, to obtain the geometry from plastic deformation only (i.e., after unloading), the actual kinematic constraints were 5%, 10%, 15%, 20% and 25%. The output geometries of the FE analysis using those constraints were later considered to be the ones coming from the crushing of 10%, 20%, 30%, 40% and 50%.

For the FE analysis the Abaqus Unified FEA from Dassault Systems was used, in which 4-node general-purpose shell finite elements were utilized (S4 according to [34]). Single model had about 3280 shell elements with linear shape functions and about 3160 nodes. The fluting was represented by 64 segments, since this value is important to retrieve

the correct transvers shear stiffnesses of a representative volume element (RVE) as shown by our recent work [25]. Here, the number of segments was doubled due to modelling contact between the top liner vs. fluting and fluting vs. bottom liner. In tangential direction, the frictionless contact was assumed; and in normal direction the Herz type contact was assumed. Boundary conditions allowed to deform the RVE in out of plane direction, blocking from movement the external (side) nodes.

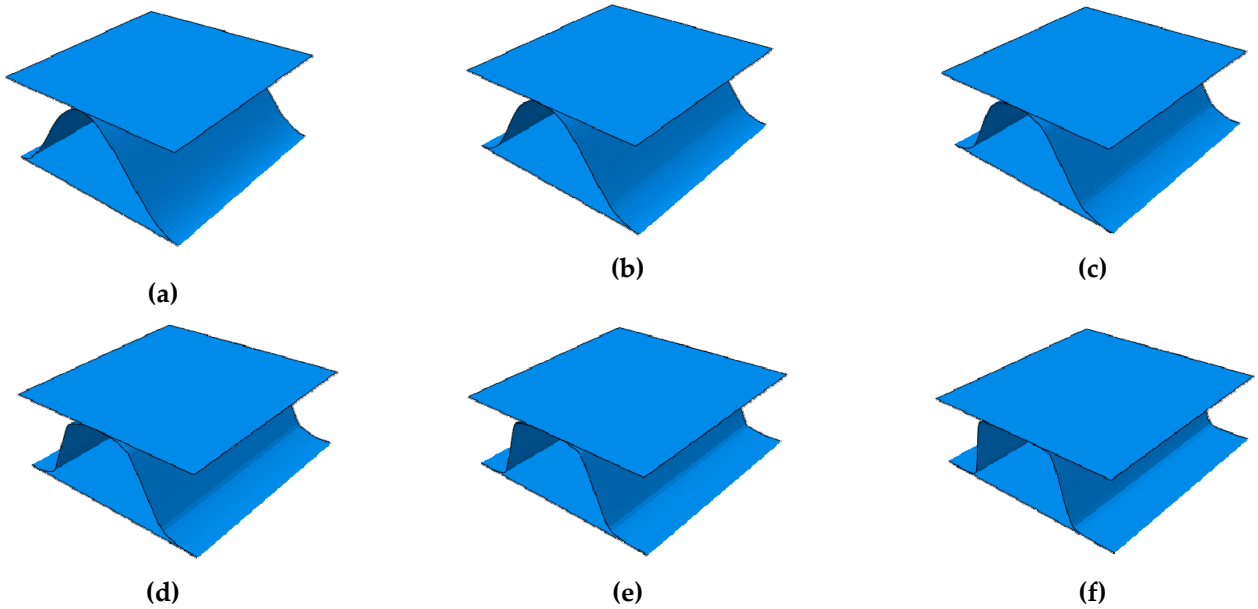

Figure 7. The crushed geometries of the corrugated cardboard obtained from the static finite element analysis: (**a**) 0%, (**b**) 10%, (**c**) 20%, (**d**) 30%, (**e**) 40% and (**f**) 50%.

Based on FEM computations performed to obtain different crushing levels, the alternative approach may be used to determine the crushing shapes of fluting to reconstruct its crushed geometry (this is valid for different flute amplitudes and periods). The analytical formula is proposed here, which accounts for the vertical coordinates of a half-wave fluting:

$$f(x) = ts\left(\frac{1}{1+e^{-2wx/L}} - \frac{1}{2}\right) \tag{4}$$

in which t is the amplitude of intact fluting, L is the period length of intact fluting, x is the horizontal coordinate, w is the parameter related to inclination and curviness of the fluting vertical wall, while s is the parameter scaling the crushing thickness; w and s should be used to fit the fluting shape to particular level of crushing. The parameters of w and s for cases used in this study are summarized in Table 2. The fluting shapes of half-waves for different crushing levels obtained from the formula proposed are presented in Figure 8a. It should be noted that the fluting length in the analytical approach was preserved by reproducing the geometry from FE analyses. The example of comparison between the fluting shape computed with the FE model and the analytical formula for 40% of crushing is presented in Figure 8b; a perfect agreement can be observed.

In the next stage of the study, the output geometries (without any residual stresses) were imported to Abaqus software to build the initial material stiffness matrix of the structure, see Figure 6c–d. Before this, for each case, namely, crushing of 10%, 20%, 30%, 40% and 50%, the geometries were inspected in order to determine which regions of the fluting were actually plasticized. For those finite element models (along CD), all elastic properties (apart Poisson's ratio) were deteriorated by scaling factor. Two regions of fluting were distinguished for each case; thus, two scaling factors were considered, see Figure 9. The first region is the contacting area of liners and fluting (region A) and the second

region is in span, which clearly would evolve into the plastic joint (region B) for larger crushing loads. The elements, in which the material was identified to be plasticized, i.e., regions A and B, were obtained from FE computations, see Figure 9. Since 50% of the deformation was assumed to be elastic, new geometries for further computations with 50% less crushing were generated by f function, see Equation (4), but in A and B regions the material properties were deteriorated.

Table 2. Geometrical parameters of w and s for fluting to determine analytically the crushed geometries of corrugated cardboard used in the numerical part of this study.

Crushing (%)	w (-)	s (-)
0 (intact)	3.5	1.06
10	4.0	0.98
20	4.8	0.92
30	6.2	0.86
40	9.0	0.80
50	15.5	0.75

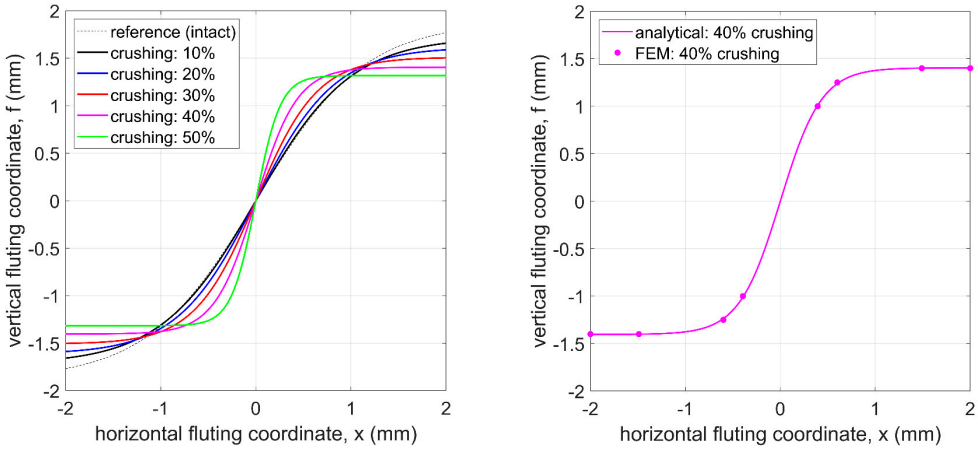

(**a**) (**b**)

Figure 8. Half-waves of fluting due to crushing obtained from the analytical formula (4) and parameters presented in Table 2: (**a**) shapes of the flute corresponding to different levels of crushing and (**b**) the comparison for 40% of crushing: FEM (magenta circles) vs analytical formula (solid line).

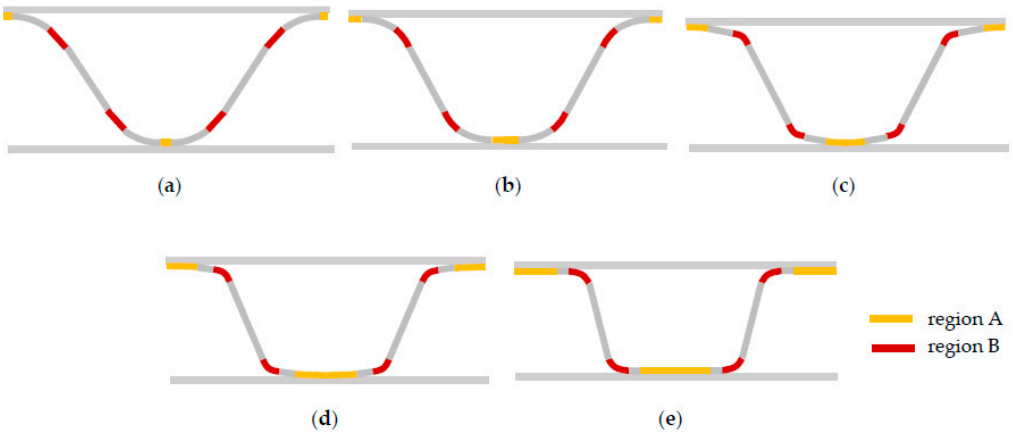

Figure 9. A and B regions for all geometries of corrugated cardboard considered, i.e., with crushing of (**a**) 10%, (**b**) 20%, (**c**) 30%, (**d**) 40% and (**e**) 50%.

The local material deterioration was defined independently for two regions: A and B. Acquired material stiffness matrix of RVE with embedded orthotropic and locally

deteriorated properties (due to decreasing of elastic properties for two regions by scaling factor) were subjected to Garbowski and Gajewski homogenization method [25], see Figure 6d,e. The method based on the stiffness matrix of the RVE enables computing $\mathbf{A}_k$ matrix, which is the overall stiffness matrix for the laminate shell element. The great advantage of the method is that it captures also the effective transvers shear stiffnesses in CD and MD of the input RVE structure, i.e., A_{44} and A_{55}, respectively.

To summarize, the overall algorithm presented in this subsection enables to compute the representative transvers shear stiffnesses for corrugated cardboard samples with different intensity of its crushing included. Results section will prove that the torsion test may be used to effectively validate this algorithm to determine the local deterioration of a corrugated board sample with particular intensity of the crushing.

3. Results

3.1. Experimental Study

In the experimental part of our study, four corrugated boards of different grammage were selected and tested, namely, two B flutes: 285 g/m^2, (B-285), 410 g/m^2 (B-410) and two C flutes: 340 g/m^2 (C-340), 440 g/m^2 (C-440). Those corrugated boards were subjected to a series of measurements and laboratory tests to check: (a) sample thickness before and after crushing—THK and THK2; (b) sample resistance to edge crushing–ECT; (c) bending stiffness in machine direction (BNT–MD) and in cross-direction (BNT–CD); (d) shear stiffness in machine direction (SST–MD) and in cross-direction (SST–CD); and (e) torsion stiffness in machine direction (TST–MD) and in cross-direction (TST–CD). In most cases, each type of corrugated board was subjected to three to four series of tests at the same crushing level. Each corrugated board was crushed in the range of 10% to 70% of its original thickness with 10% increments. Due to the elastic relaxation of the corrugated cardboard, the measurement of the crushed sample thickness was performed a few minutes after crushing, which guaranteed initial stabilization of the relaxation of the material.

In Figures 10–13, the results of the measured parameters for the four analysed corrugated boards are presented. Based on the data, the regression lines for each test, according to Equation (2) and (3), were determined. The BNT, SST and TST values were presented in a normalized manner, the values demonstrated are the ratio of the value obtained for crushed sample to the value obtained from an intact corrugated cardboard (i.e., for CRS = 0%).

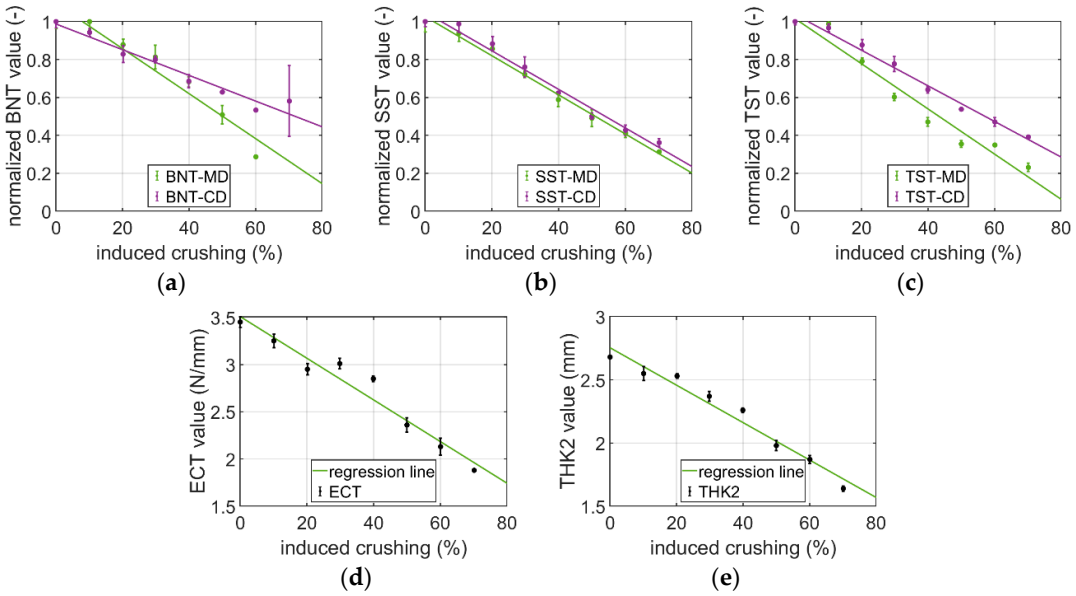

Figure 10. The decreases in measured values for B-285 corrugated cardboard in: (**a**) BNT; (**b**) SST; (**c**) TST; (**d**) ECT and (**e**) THK2.

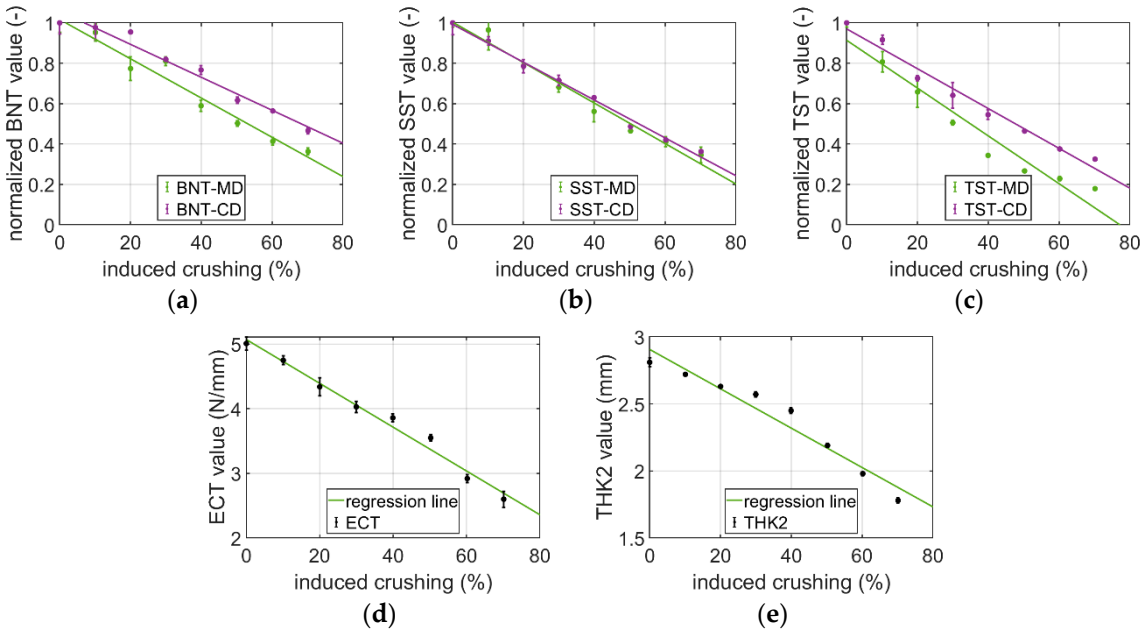

Figure 11. The decreases in measured values for B-410 corrugated cardboard in: (**a**) BNT; (**b**) SST; (**c**) TST; (**d**) ECT and (**e**) THK2.

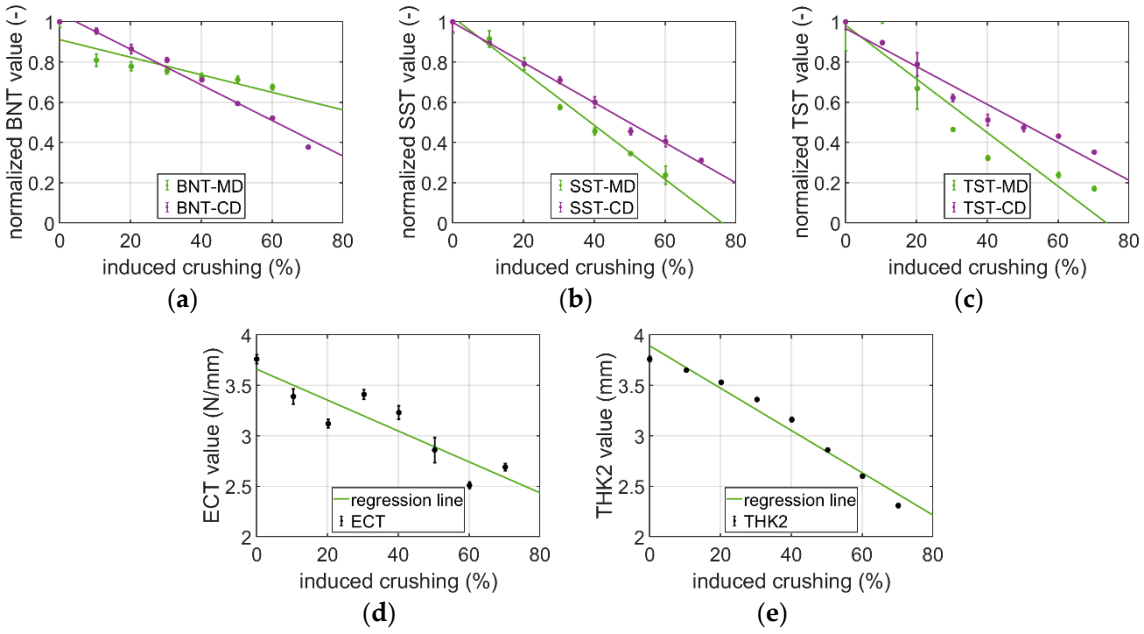

Figure 12. The decreases in measured values for C-340 corrugated cardboard in: (**a**) BNT; (**b**) SST; (**c**) TST; (**d**) ECT and (**e**) THK2.

The relationship between crushing and decrease of parameter values was investigated by computing the coefficient of determination for each quantity, according to Equation (1). In Table 3, the values obtained are presented.

Determining the crushing level from the stiffness tests is more precise when the average values from the MD and CD are used to compute the linear regression. This fact may be observed in Figure 14, in which the normalized parameter values were averaged from two directions and the crushing lines are shown. In Table 4, the corresponding coefficients of determination for the averaged values from two directions are presented.

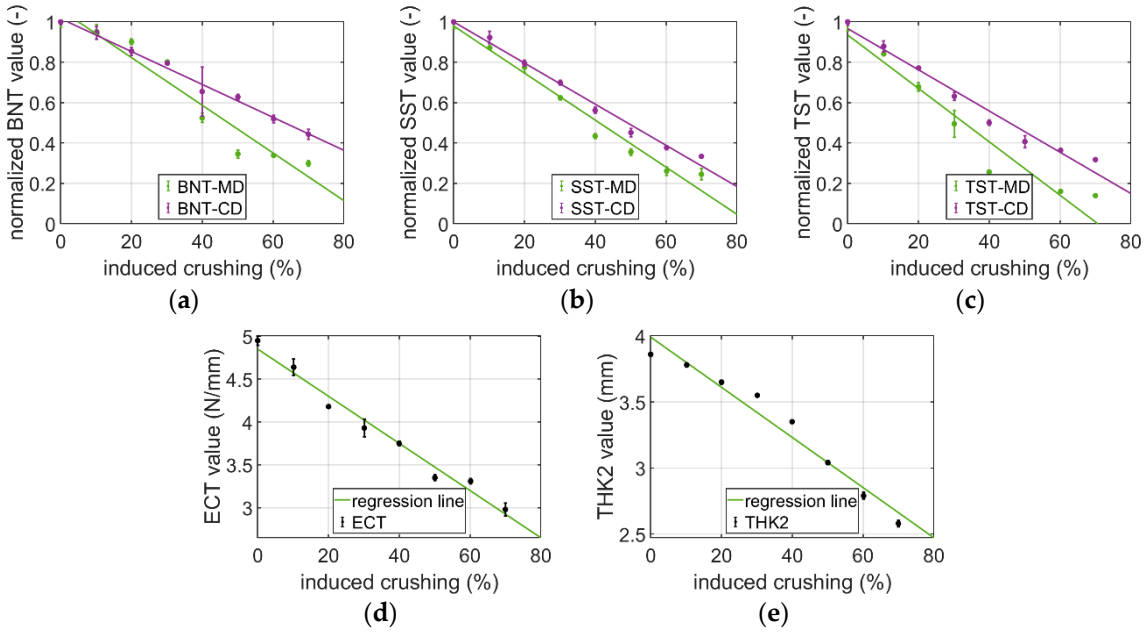

Figure 13. The decreases in measured values for C-440 corrugated cardboard in: (**a**) BNT; (**b**) SST; (**c**) TST; (**d**) ECT and (**e**) THK2.

Table 3. The coefficient of determination R^2 between crushing and normalized values.

Cardboard Index	THK2	ECT	BNT-MD	BNT-CD	SST-MD	SST-CD	TST-MD	TST-CD
B-285	0.154	0.481	0.928	0.705	0.995	0.964	0.914	0.932
B-410	0.001	0.596	0.986	0.687	1.000	0.992	0.535	0.988
C-340	0.111	0.016	0.517	0.861	0.719	1.000	0.542	0.993
C-440	0.000	0.452	0.967	0.841	0.855	0.999	0.290	0.968

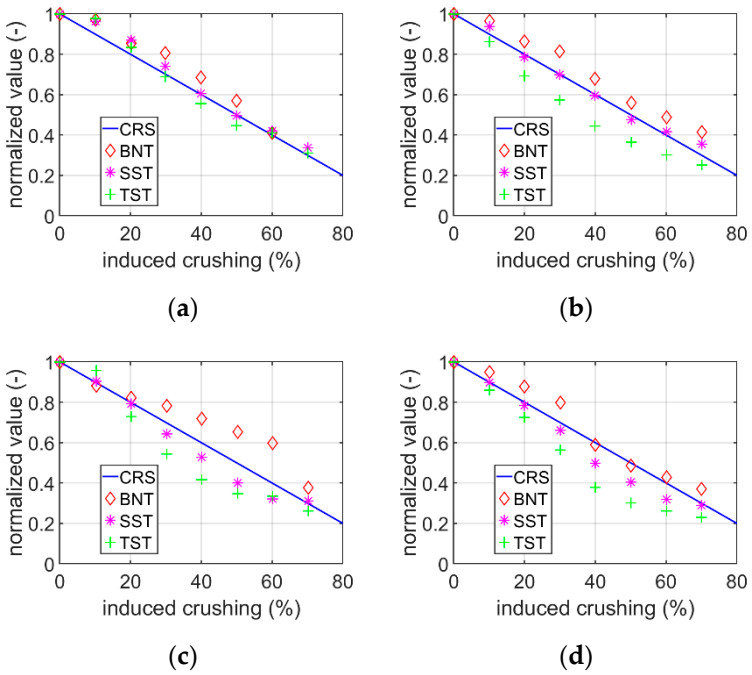

Figure 14. The decreases in measured values (average from two directions) for corrugated board with an index: (**a**) B-285; (**b**) B-410; (**c**) C-340 and (**d**) C-440.

Table 4. The coefficient of determination R^2 between crushing and average normalized values.

Cardboard Index	BNT	SST	TST
B-285	0.823	0.983	0.996
B-410	0.885	0.998	0.846
C-340	0.815	0.970	0.876
C-440	0.972	0.957	0.742

We found that there is a relationship between the decreased ECT and THK2 value. A reference line, which capture the relationship between the decrease of these normalized parameters and crushing of the corrugated cardboard was established. The equation describing the reference line has a following form:

$$y = 1 - 0.53x \tag{5}$$

where: y—the normalized parameter value and x—the crushing value.

In Figure 15, the normalized ECT and THK2 values for the analysed corrugated cardboards fitting to the reference lines represented by the Equation (5) are presented.

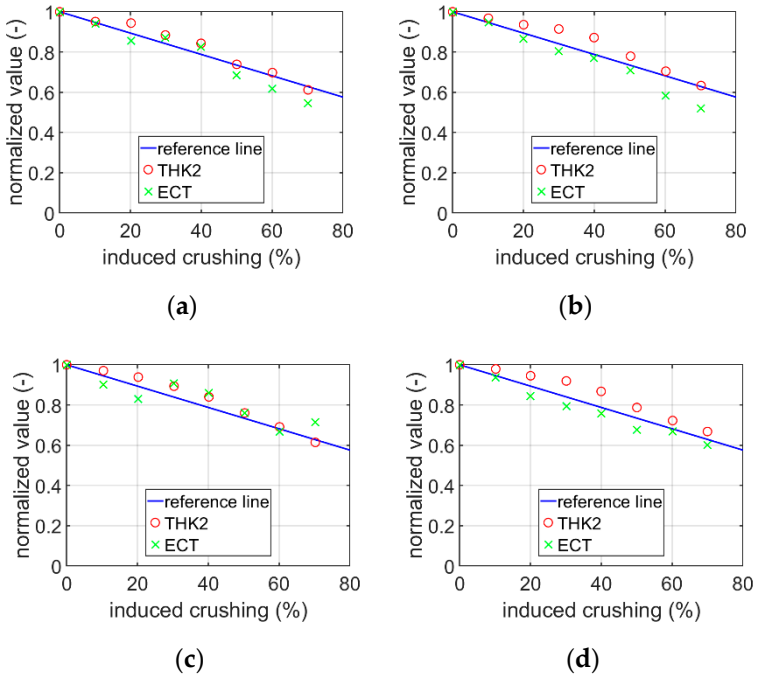

Figure 15. The decreases in normalized ECT and THK2 values for corrugated board with an index: (**a**) B-285; (**b**) B-410; (**c**) C-340 and (**d**) C-440.

For the reference line and normalized ECT and THK2 values, the coefficients of determination R^2 were computed (Table 5), according to Equation (1) for the two sets of data simultaneously, where: x_i—reference line value calculated from the Equation (5), $\hat{y}_i$—normalized ECT and THK2 values and $\mathrm{var}(x)$—variance of the reference line value.

Table 5. The coefficient of determination R^2 between reference line and normalized ECT and THK2 values.

Cardboard Index	R^2
B-285	0.985
B-410	0.982
C-340	0.965
C-440	0.995

3.2. Numerical Appraoch for Modelling Crushing

The shell stiffnesses ($\mathbf{A}_k$ matrix) were computed for five crushing levels of corrugated cardboard considered, i.e., with different amount of crushing: 10%, 20%, 30%, 40% and 50%. The local deterioration factor for region A was assumed 0.5 and for region B was assumed 0.9 (due to severe delamination in these regions as shown by [35,36]). Selected values of $\mathbf{A}_k$ matrices for different level of crushing were presented in Table 6.

Table 6. The stiffnesses of the representative shell element computed for different crushing of corrugated cardboard sample for local deterioration scaling factors, separately for region A and region B.

Stiffness	10% Crushing	20% Crushing	30% Crushing	40% Crushing	50% Crushing
A_{11}, $(\mathrm{kPa}\cdot\mathrm{m})$	2101.4	2092.8	2088	2085.3	2078.7
A_{22}, $(\mathrm{kPa}\cdot\mathrm{m})$	1591.5	1568.1	1548.5	1531.6	1477.4
A_{12}, $(\mathrm{kPa}\cdot\mathrm{m})$	371.3	367.8	365.5	363.8	361.5
A_{33}, $(\mathrm{kPa}\cdot\mathrm{m})$	603.0	586.3	573.4	562.3	543.9
D_{11}, $(\mathrm{Pa}\cdot\mathrm{m}^3)$	5.79	5.19	4.64	4.11	3.61
D_{22}, $(\mathrm{Pa}\cdot\mathrm{m}^3)$	3.6	3.23	2.89	2.57	2.21
D_{12}, $(\mathrm{Pa}\cdot\mathrm{m}^3)$	1.01	0.90	0.81	0.71	0.63
D_{33}, $(\mathrm{Pa}\cdot\mathrm{m}^3)$	1.50	1.34	1.19	1.06	0.92
A_{44},$(\mathrm{Pa}\cdot\mathrm{m})$	45.18	31.12	22.01	15.41	10.14
A_{55}, $(\mathrm{Pa}\cdot\mathrm{m})$	82.13	72.55	65.58	60.11	51.45

Having computed $\mathbf{A}_k$ stiffnesses which represents the overall material properties of RVE, the values were used to determine the behavior of the corrugated cardboard samples from different tests. Torsion and bending stiffness tests in both directions were considered here, see its analytical formulas derived in [31,32]. The dimension of the torsion sample was 80 × 80 mm, in bending the sample had 100 mm length between the internal supports. The decreases of stiffness of the corrugated sample in the cases of torsion, bending in CD and bending in MD for assumed scaling factors (see non deteriorated values in Table 1) are presented in Table 7. It may be observed that the values are close to the induced crushing values (first column), especially for torsion test (second column), what proves that the method was validated. This method may be used in other applications for modelling crushed corrugated cardboard samples for deriving its material and mechanical properties.

Table 7. The decreases in stiffness of torsion, bending in CD and bending in MD for scaling factors separately identified for region A and region B – obtained for different input geometry due to induced crushing (see Figure 9).

Induced Crushing (%)	Torsion Stiffness Decrease (%)	CD Bending Stiffness Decrease (%)	MD Bending Stiffness Decrease (%)
10	12	10	12
20	21	19	21
30	30	28	29
40	38	36	37
50	46	44	46

4. Discussion

In the first part of our work, we investigated the relationship between the intentional level of flat corrugated cardboard crushing and the drops in the measured parameters of various laboratory tests. The results in Tables 4 and 5 show the coefficients of determination for linear trends (y = x) across all tests. Values closer to 1 indicate the better correlation between the experiment result and the regression lines. It has been observed that the decrease in both bending and torsional stiffness is more or less correlated with the amount of crush.

The results obtained show that the SST parameters best catch the amount of intentional crushing, the TST parameters are slightly worse and the BNT parameters are the least accurate. Mean coefficients of determination for all four corrugated board types were: SST—0.977; TST—0.874, BNT—0.865. The correlation of crush amount with the results of the SST tests at the level of 97.7% means that if there is a need to check a posteriori the amount of the unknown damage caused by the converting machines, it is sufficient to measure the SST parameter before and after the converting process and its ratio will indicate the crushing level. This is because the amount of decrease of the SST parameter precisely reflects the degree of corrugated board crushing. The decrease in the parameter measured in SST does not depend on the residual thickness of the crushed corrugated cardboard, which often returns to its original value due to relaxation. Therefore, organoleptic inspection (e.g., measuring thickness) often does not reveal the problem hidden inside the delaminated cardboard fibers. Therefore, the new insight from this part of study is the following: one may use shearing test (SST) for determining the crushing level of the single wall cardboard, other tests such as bending or torsion are less indicative. This conclusion opens new possibilities to design similar test/machines in other types of materials in which crushing is observed and unwanted, for instance in civil engineering or automotive industry.

On the other hand, the drop in ECT parameter and the residual thickness, THK2 correlate well with each other. The measured thickness after crushing decreases almost by the same value as the measured ECT value (again after crushing). The amount of deterioration of measured ECT and the permanent thickness reduction is approximately 50% of the actual crush amount of the corrugated board. Thus, thickness/ECT reduction may be used to roughly estimate the amount of crushing in a single wall corrugated boards but is not recommended for cases in which high accuracy is expected.

In the numerical part of the study, the results show that the numerical procedure presented can reproduce the deterioration of the samples stiffnesses due to crushing by decreasing the elastic parameters of the RVE, see Table 6. The regions for which the deterioration must be included were identified as the contacting area of liners and fluting (region A) and in the span area (region B), see Figure 9, also the deterioration factors were acquired, i.e., 0.5 for region A and 0.9 for region B. This property seems to be significantly important if one would like to compute the deteriorated properties of the cardboard, basing only on its crushed shape and knowing intact properties of the corrugated cardboard ($\mathbf{A}_k$ matrix). As shown, by introducing the analytical formulation, Equation (4), with adequate parameters, see Table 2, to determine the crushed shape one does not have to perform costly FE analysis [37,38], nor have to use advanced (plastic) material constitutive models, see Figure 6. The analytical formulation may be therefore adopted in optimization or inverse problem frameworks, in which computational cost should be limited.

It should be underlined that the numerical study presented enables obtaining the transversal shear stiffness properties of the sample by using the torsion test for different levels of crushing, see Table 6. This is extremely important since the crushing of the cardboard is often suspected to cause the biggest amount of unintended decrease of the load capacity of corrugated cardboard boxes. However, up to this point, there are no systematic and implemented in the industry methods that would be able to determine how the crushing influences the deterioration of the transversal shear stiffnesses. Thus, if this phenomenon may be modelled easily, by the procedure proposed (without using FE computations, nor advanced material models, but adopting an analytical/algebraic rapid and versatile approach), we are one step closer to deliver the scientific-based methodology for dealing with the crushing issue for the corrugated board packaging industry.

5. Conclusions

The article presents extended laboratory tests of single-walled corrugated cardboard, consisting in checking the impact of crushing on its mechanical properties. The intentional crushing of the cross-section from 10 to 70% of the original height was fully controlled and initiated with high precision. During the tests, a number of parameters of the corrugated

board were measured, i.e., (a) residual thickness after elastic relaxation, (b) decrease in bending stiffness, (c) decrease in torsional stiffness, (d) decrease in shear stiffness and (e) decrease in edge crush strength. The reduction in stiffness was checked in two mutually perpendicular directions (i.e., in machine direction and cross direction), while the strength reduction was checked in cross direction only. A correlation was found between intentional and controlled crushing and the corresponding reduced stiffness. It was observed that the best match between the amount of crush and the reduction in stiffness for all specimens tested occurred in the shear stiffness test (SST). The paper also presents numerical and analytical tools for quick and reliable calculations of degraded stiffness of crushed corrugated cardboard samples. For selected crushing levels of the corrugated cardboards the stiffnesses of the representative volume elements were computed. In further research, the impact of the crushing of corrugated board for double-walled structures on the packaging performance will be studied.

Author Contributions: Conceptualization, T.G. (Tomasz Garbowski) and T.G. (Tomasz Gajewski); methodology, T.G. (Tomasz Garbowski); software, T.G. (Tomasz Gajewski) and D.M.; validation, T.G. (Tomasz Garbowski), T.G. (Tomasz Gajewski) and D.M.; formal analysis, T.G. (Tomasz Garbowski), T.G. (Tomasz Gajewski) and D.M.; investigation, T.G. (Tomasz Garbowski), T.G. (Tomasz Gajewski), D.M. and R.J.; writing—original draft preparation, T.G. (Tomasz Garbowski), T.G. (Tomasz Gajewski) and D.M.; writing—review and editing, T.G. (Tomasz Garbowski), T.G. (Tomasz Gajewski) and R.J.; visualization, T.G. (Tomasz Gajewski) and D.M.; supervision, T.G. (Tomasz Garbowski); project administration, T.G. (Tomasz Garbowski); funding acquisition, R.J. All authors have read and agreed to the published version of the manuscript.

Funding: The APC was funded by the National Center for Research and Development, Poland, grant at Werner Kenkel Sp z o. o., grant number POIR.01.01.01–00-1306/15–00.

Institutional Review Board Statement: Not applicable.

Informed Consent Statement: Not applicable.

Data Availability Statement: The data presented in this study are available on request from the corresponding author.

Acknowledgments: The authors thank AQUILA VPK Wrzesnia for providing samples of corrugated cardboard for the study. The authors also thank to Femat Sp. z o. o. for providing the laboratory equipment and commercial software.

Conflicts of Interest: The authors declare no conflict of interest. The funders had no role in the design of the study; in the collection, analyses or interpretation of data; in the writing of the manuscript or in the decision to publish the results.

References

1. Kellicutt, K.; Landt, E. Development of design data for corrugated fiberboard shipping containers. *Tappi J.* **1952**, *35*, 398–402.
2. Maltenfort, G. Compression strength of corrugated containers. *Fibre Contain.* **1956**, *41*, 106–121.
3. McKee, R.C.; Gander, J.W.; Wachuta, J.R. Compression strength formula for corrugated boxes. *Paperb. Packag.* **1963**, *48*, 149–159.
4. Buchanan, J.S.; Draper, J.; Teague, G.W. Combined board characteristics that determine box performance. *Paperb. Packag.* **1964**, *49*, 74–85.
5. Shick, P.E.; Chari, N.C.S. Top-to-bottom compression for double wall corrugated boxes. *Tappi J.* **1965**, *48*, 423–430.
6. Wolf, M. New equation helps pin down box specifications. *Packag. Eng.* **1972**, *17*, 66–67.
7. Allerby, I.M.; Laing, G.N.; Cardwell, R.D. Compressive strength—From components to corrugated containers. *Appita Conf. Notes* **1985**, 1–11.
8. Schrampfer, K.E.; Whitsitt, W.J.; Baum, G.A. *Combined Board Edge Crush (ECT) Technology*; Institute of Paper Chemistry: Appleton, WI, USA, 1987.
9. Batelka, J.J.; Smith, C.N. *Package Compression Model*; Institute of Paper Science and Technology: Atlanta, GA, USA, 1993.
10. Urbanik, T.J.; Frank, B. Box compression analysis of world-wide data spanning 46 years. *Wood Fiber Sci.* **2006**, *38*, 399–416.
11. Biancolini, M.E.; Brutti, C.; Porziani, S. Corrugated board containers design methods. In Proceedings of the Associazione Italiana per l'Analisi delle Sollecitazioni (AIAS) XXXVI Convegno Nazionale 2007, Naples, Italy, 4–8 September 2007.
12. Han, J.; Park, J.M. Finite element analysis of vent/hand hole designs for corrugated fibreboard boxes. *Packag. Technol. Sci.* **2007**, *20*, 39–47. [CrossRef]

13. Garbowski, T.; Jarmuszczak, M. Numerical strength estimate of corrugated board packages. Part 1. Theoretical assumptions in numerical modeling of paperboard packages. *Pol. Pap. Rev.* **2014**, *70*, 219–222. (In Polish)
14. Garbowski, T.; Jarmuszczak, M. Numerical strength estimate of corrugated board packages. Part 2. Experimental tests and numerical analysis of paperboard packages. *Pol. Pap. Rev.* **2014**, *70*, 277–281. (In Polish)
15. Fadiji, T.; Coetzee, C.J.; Opara, U.L. Compression strength of ventilated corrugated paperboard packages: Numerical modelling, experimental validation and effects of vent geometric design. *Biosyst. Eng.* **2016**, *151*, 231–247. [CrossRef]
16. Fadiji, T.; Ambaw, A.; Coetzee, C.J.; Berry, T.M.; Opara, U.L. Application of the finite element analysis to predict the mechanical strength of ventilated corrugated paperboard packaging for handling fresh produce. *Biosyst. Eng.* **2018**, *174*, 260–281. [CrossRef]
17. Hohe, J. A direct homogenization approach for determination of the stiffness matrix for microheterogeneous plates with application to sandwich panels. *Compos. Part B* **2003**, *34*, 615–626. [CrossRef]
18. Buannic, N.; Cartraud, P.; Quesnel, T. Homogenization of corrugated core sandwich panels. *Compos. Struct.* **2003**, *59*, 299–312. [CrossRef]
19. Biancolini, M.E. Evaluation of equivalent stiffness properties of corrugated board. *Compos. Struct.* **2005**, *69*, 322–328. [CrossRef]
20. Abbès, B.; Guo, Y.Q. Analytic homogenization for torsion of orthotropic sandwich plates: Application. *Compos. Struct.* **2010**, *92*, 699–706. [CrossRef]
21. Garbowski, T.; Jarmuszczak, M. Homogenization of corrugated paperboard. Part 1. Analytical homogenization. *Pol. Pap. Rev.* **2014**, *70*, 345–349. (In Polish)
22. Garbowski, T.; Jarmuszczak, M. Homogenization of corrugated paperboard. Part 2. Numerical homogenization. *Pol. Pap. Rev.* **2014**, *70*, 390–394. (In Polish)
23. Garbowski, T.; Marek, A. Homogenization of corrugated boards through inverse analysis. In Proceedings of the 1st International Conference on Engineering and Applied Sciences Optimization, Kos Island, Greece, 4–6 June 2014; pp. 1751–1766.
24. Marek, A.; Garbowski, T. Homogenization of sandwich panels. *Comput. Assist. Methods Eng. Sci.* **2015**, *22*, 39–50.
25. Garbowski, T.; Gajewski, T. Determination of transverse shear stiffness of sandwich panels with a corrugated core by numerical homogenization. *Materials* **2021**, *14*, 1976. [CrossRef] [PubMed]
26. Suarez, B.; Muneta, M.L.M.; Sanz-Bobi, J.D.; Romero, G. Application of homogenization approaches to the numerical analysis of seating made of multi-wall corrugated cardboard. *Compos. Struct.* **2021**, *262*, 113642. [CrossRef]
27. Garbowski, T.; Gajewski, T.; Grabski, J.K. The role of buckling in the estimation of compressive strength of corrugated cardboard boxes. *Materials* **2020**, *13*, 4578. [CrossRef] [PubMed]
28. Garbowski, T.; Gajewski, T.; Grabski, J.K. Estimation of the compressive strength of corrugated cardboard boxes with various openings. *Energies* **2021**, *14*, 155. [CrossRef]
29. Garbowski, T.; Gajewski, T.; Grabski, J.K. Estimation of the compressive strength of corrugated cardboard boxes with various perforations. *Energies* **2021**, *14*, 1095. [CrossRef]
30. Nordstrand, T.; Carlsson, L. Evaluation of transverse shear stiffness of structural core sandwich plates. *Compos. Struct.* **1997**, *37*, 145–153. [CrossRef]
31. Garbowski, T.; Gajewski, T.; Grabski, J.K. Torsional and transversal stiffness of orthotropic sandwich panels. *Materials* **2020**, *13*, 5016. [CrossRef] [PubMed]
32. Garbowski, T.; Gajewski, T.; Grabski, J.K. Role of transverse shear modulus in the performance of corrugated materials. *Materials* **2020**, *13*, 3791. [CrossRef] [PubMed]
33. FEMat Systems. Available online: http://fematsystems.pl/home_en/ (accessed on 26 April 2021).
34. Abaqus Unified FEA Software. Available online: https://www.3ds.com/products-services/simulia/products/abaqus (accessed on 26 April 2021).
35. Jamsari, M.A.; Kueh, C.; Gray-Stuart, E.M.; Dahm, K.; Bronlund, J.E. Modelling the impact of crushing on the strength performance of corrugated fibreboard. *Packag Technol. Sci.* **2020**, *33*, 159–170. [CrossRef]
36. Jamsari, M.A.; Kueh, C.; Gray-Stuart, E.; Martinez-Hermosilla, G.A.; Dahm, K.; Bronlund, J.E. A technique to quantify morphological damage of the flute profile in the midplane of corrugated fibreboard. *Packag. Technol. Sci.* **2019**, *32*, 213–226. [CrossRef]
37. Jamsari, M.A.; Kueh, C.; Gray-Stuart, E.M.; Dahm, K.; Bronlund, J.E. Experimental and numerical performance of corrugated fibreboard at different orientations under, four-point bending test. *Packag Technol Sci.* **2019**, *32*, 555–565. [CrossRef]
38. Park, J.; Park, M.; Choi, D.S.; Jung, H.M.; Hwang, S.W. Finite element-based simulation for edgewise compression behavior of corrugated paperboard for packing of agricultural products. *Appl. Sci.* **2020**, *10*, 6716. [CrossRef]